Formation Mechanism of Fullerene Cation in Bulk Heterojunction Polymer Solar Cells

Shunsuke Yamamoto, Hideo Ohkita, Hiroaki Benten, and Shinzaburo Ito*

The charge carrier dynamics in blend films of [6,6]-phenyl-C_{61}-butyric acid methyl ester (PCBM) and conjugated polymers with different ionization potentials are measured using transient absorption spectroscopy to study the formation mechanism of PCBM radical cation, which was previously discovered for blend films of poly[2-methoxy-5-(3,7-dimethyloctyloxy)-1,4-phenylenevinylene] (MDMO-PPV) and PCBM. On a nanosecond time scale after photoexcitation, polymer hole polaron and PCBM radical anion are observed but no PCBM radical cation is found in the blends. Subsequently, the fraction of polymer hole polarons decreases and that of PCBM radical cations increases with time. Finally, the fraction of PCBM radical cations becomes constant on a microsecond time scale. The final fraction of PCBM radical cation is dependent on the ionization potential of polymers but independent of the excitation wavelength. These findings show that the formation of PCBM radical cation is due to hole injection from polymer to PCBM domains. Furthermore, the energetic conditions for such hole injection in polymer/PCBM blend films are discussed on the basis of Monte Carlo analysis for hole hopping in a disordered donor/acceptor heterojunction with varying energetic parameters.

1. Introduction

In polymer/fullerene solar cells, semiconducting conjugated polymers and fullerene derivatives are generally considered to serve as a hole-transporting and electron-transporting materials, respectively.[1,2] Indeed, organic semiconductors with a shallow ionization potential tend to be p-type semiconductors and organic semiconductors with a deep ionization potential tend to be n-type semiconductors. On the other hand, ambipolar transport properties have been recently reported for not a few materials including fullerenes, pentacene, and conjugated polymers in the field effect transistor (FET) devices with appropriate electrodes and gate dielectrics.[3–8] These reports indicate that organic semiconducting materials are inherently capable to be ambipolar.[9]

Recently, there have been several studies indicative of ambipolar charge transport of fullerene derivatives even in polymer/fullerene blends. For blend films of poly[2-methoxy-5-(3,7-dimethyloctyloxy)-1,4-phenylenevinylene] (MDMO-PPV) and [6,6]-phenyl-C_{61}-butyric acid methyl ester (PCBM), the hole mobility increases as the increase in the PCBM fraction. The hole mobility of MDMO-PPV/PCBM blend films ($2–3 \times 10^{-4}$ cm^2 V^{-1} s^{-1})[10,11] is at least two orders of magnitude larger than that of a pristine MDMO-PPV film ($0.3–2 \times 10^{-6}$ cm^2 V^{-1} s^{-1}),[10,11] but rather comparable to the FET hole mobility of PCBM (8×10^{-3} cm^2 V^{-1} s^{-1}).[6] For blend films of poly[2,7-(9,9-dioctylfluorene)-*alt*-5,5-(5′,8′-di-2-thienyl-(2′,3′-bis-(3″-octyloxyphenyl)-quinoxaline))] (APFO-15) and PCBM, the electroluminescence of PCBM emission has been observed in addition to that of charge transfer (CT) emission.[12] These findings suggest hole transport in the fullerene phase in polymer/fullerene blends. Previously, we found the formation of fullerene radical cation in MDMO-PPV/PCBM blend films by transient absorption measurements: no PCBM radical cation is observed at low PCBM concentrations while PCBM radical cation is observed in addition to PCBM radical anion at high PCBM concentrations.[13] This is consistent with previous reports that the hole mobility in MDMO-PPV/PCBM blend films increases at higher PCBM concentrations (>50 wt%).[11] However, little is known about the formation mechanism of fullerene radical cation in polymer/fullerene blends.

Herein, we systematically study the charge carriers formed in blend films of PCBM and conjugated polymers with different ionization potentials in order to address the formation mechanism of fullerene radical cation in polymer/fullerene blends. **Figure 1** shows conjugated polymers employed in this study: poly[2,6-(4,4-bis-(2-ethylhexyl)-4*H*-cyclopenta[2,1-b;3,4-b′]dithiophene)-*alt*-4,7(2,1,3-benzothiadiazole)] (PCPDTBT) and poly[2,7-(9,9-dioctylfluorene)-*alt*-5,5-(5′,8′-di-2-thienyl-2′,3′-diphenylquinoxaline)] (N-P7). PCPDTBT and N-P7 have smaller or similar ionization potential (I_p = 4.9 eV for PCPDTBT[14] and 5.37 eV for N-P7[15]) compared to MDMO-PPV (I_p = 5.4 eV[16]). Furthermore, polymer solar cells with them exhibit the

S. Yamamoto, Dr. H. Ohkita,
Dr. H. Benten, Prof. S. Ito
Department of Polymer Chemistry
Graduate School of Engineering
Kyoto University
Katsura, Nishikyo, Kyoto 615-8510, Japan
E-mail: ohkita@photo.polym.kyoto-u.ac.jp
Dr. H. Ohkita
Japan Science and Technology Agency (JST)
PRESTO, 4-1-8 Honcho Kawaguchi
Saitama 332-0012, Japan

DOI: 10.1002/adfm.201200086

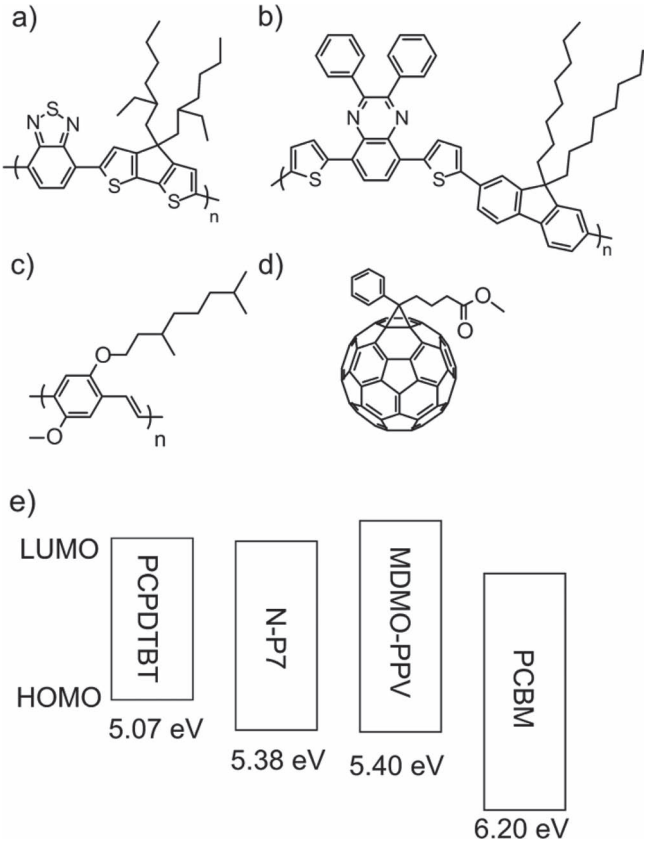

Figure 1. Chemical structures of conjugated polymers and a fullerene employed in this study: a) PCPDTBT, b) N-P7, c) MDMO-PPV, and d) PCBM. e) The energy diagrams of these materials. The HOMO energy is measured by the photoelectron yield spectroscopy (see the Supporting Information).

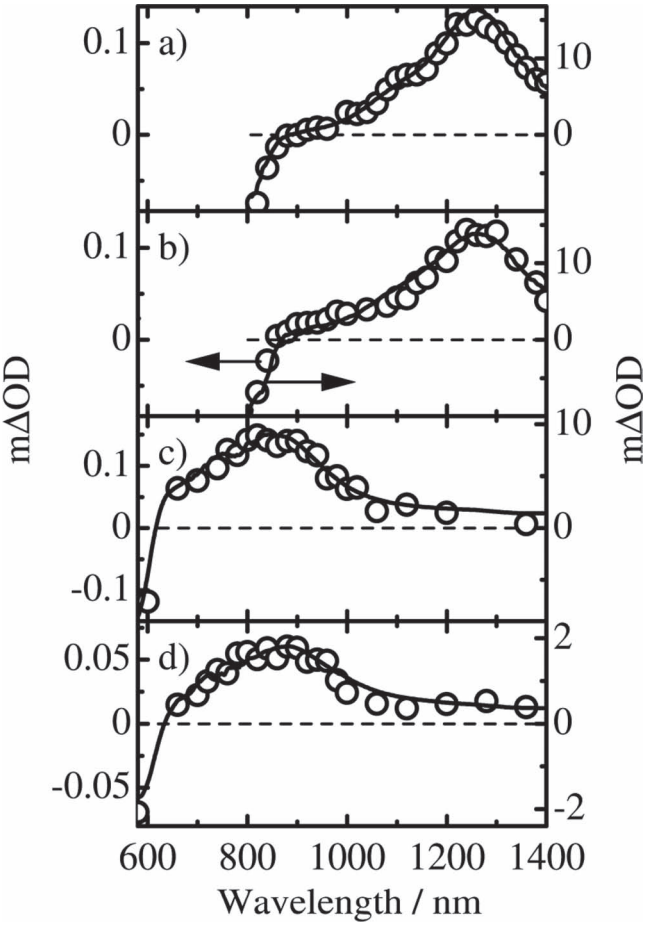

Figure 2. Transient absorption spectra of blend films: a) PCPDTBT/TCNB (95:5 w/w), b) PCPDTBT/TCNB (70:30 w/w), c) N-P7/TCNB (95:5 w/w), and d) N-P7/TCNB (70:30 w/w). The solid lines and open circles show the spectra measured at 3 ns and 0.5 μs after the laser excitation, respectively. The broken lines represent the baseline.

optimized power conversion efficiency (~5.5%) at high weight fractions of fullerene (1:2 or 1:3),[17,18] as is the case of MDMO-PPV/PCBM (1:4).[19] The time evolution of PCBM radical cation formation is analyzed on the basis of the absorption coefficients of polymer polarons, PCBM radical anion, and PCBM radical cation. The formation time is dependent on polymer ionization potential and phase-separated domain size. The final fraction of PCBM radical cation F_{eq} is dependent on the polymer ionization but independent of the phase-separated domain size and the excitation wavelength. Furthermore, F_{eq} is calculated by the Monte Carlo simulation for hole injection from polymer to fullerene domains. We discuss the mechanism and energetic conditions of the formation of PCBM radical cation in polymer/PCBM blend films.

2. Results

2.1. Transient Absorption

To assign the absorption spectrum of PCPDTBT and N-P7 hole polarons, we measured transient absorption spectra of polymer films doped with tetracyanobenzene (TCNB): TCNB is a strong electron acceptor ($E_{1/2}(TCNB^-/TCNB)$ = –0.6 V vs SCE[20]) similar to C_{60} ($E_{1/2}(C_{60}^-/C_{60})$ = –0.3––0.4 V vs SCE[21]). No fluorescence was observed for the TCNB blended films, indicating that TCNB efficiently acts as an electron acceptor in the blend films. **Figure 2**a,b shows the transient absorption spectra of PCPDTBT/TCNB blend films with 5 and 30 wt% TCNB in the microsecond time region, which are almost the same as those in the nanosecond time region. A broad absorption was observed at ~1240 nm for both blend films with 5 wt% and 30 wt% TCNB. This absorption was not quenched in an oxygen atmosphere, and hence not possible to ascribe to triplet exciton. Note that TCNB radical anion has no absorption band in this wavelength region.[20] Therefore, the absorption band at 1240 nm is safely assigned to the absorption of PCPDTBT hole polaron, which is consistent with previous reports.[22,23] Figure 2c,d shows the transient absorption spectra of N-P7/TCNB blend films with 5 and 30 wt% TCNB in the microsecond time region, which are also almost the same as those in the nanosecond time region. The broad absorption band at ~850 nm is similarly ascribed to

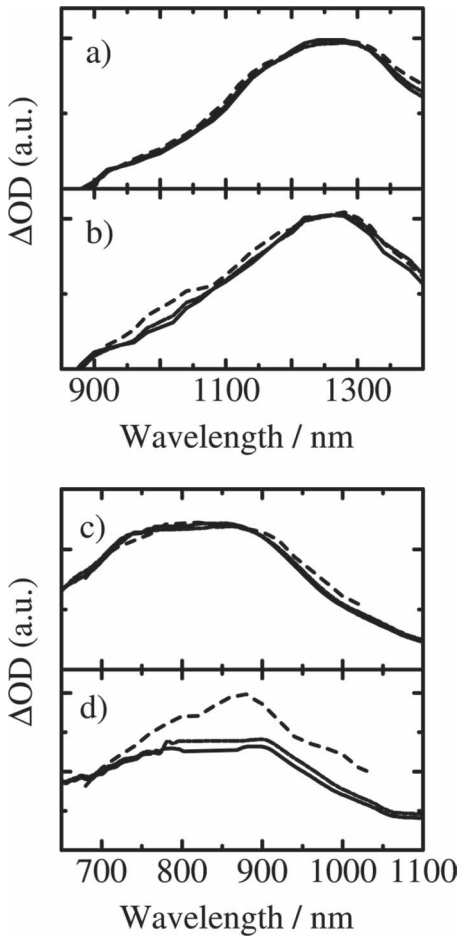

Figure 3. Transient absorption spectra of blend films excited at 400 nm with a fluence of 30 μJ cm^{-2}: a) PCPDTBT/PCBM (95:5 w/w), b) PCPDTBT/PCBM (50:50 w/w), c) N-P7/PCBM (95:5 w/w), and d) N-P7/PCBM (50:50 w/w). These spectra are normalized at a,b) 1240 nm and c,d) 700 nm. In the panels (a,b), the solid, dashed-dotted, and broken lines show the spectra at 0.5, 2, and 5 μs, respectively. In the panels (c,d), the solid, dashed-dotted, and broken lines show the spectra at 1, 3, and 500 ns, respectively.

N-P7 hole polaron. In summary, the absorption spectra of both PCPDTBT and N-P7 hole polarons are independent of time and the dopant concentration.

Figure 3 shows the transient absorption spectra of PCPDTBT/PCBM and N-P7/PCBM blend films (5 and 50 wt% of PCBM) excited at 400 nm. The absorption spectra were normalized at 1240 nm for PCPDTBT/PCBM and at 700 nm for N-P7/PCBM blends where only polymer hole polarons have an absorption band (see the supporting information). For the blend films with 5 wt% PCBM, no spectral change was observed in this time region, suggesting no change in the charge carrier composition. For the blend with 50 wt% PCBM, on the other hand, distinct spectral changes were observed for blend films: the absorption at around 1000 nm increased for PCPDTBT/PCBM and the absorption at around 900 nm increased for N-P7/PCBM. The same results were obtained upon the selective excitation of polymers: PCPDTBT at 800 nm and N-P7 at 570 nm. In other words, these temporal changes in the absorption spectra are independent of the excitation wavelength. The absorption increase at 1000 nm in PCPDTBT/PCBM blend is indicative of the increase in the fraction of the PCBM radical anion because PCBM radical anion has a characteristic absorption at 1020 nm.[13] As described below, the relative increase in the fraction of the PCBM radical anion is due to the decrease in the fraction of PCPDTBT hole polaron caused by the formation of PCBM radical cation. On the other hand, the absorption increase at 900 nm in N-P7/PCBM blends is indicative of the increase in the fraction of the PCBM radical cation because PCBM radical cation has a characteristic absorption at 890 nm, which is similar to that reported for other methanofullerene derivative cations.[13,24] In summary, both findings suggest hole injection from polymer to PCBM in blend films with high PCBM fractions as is discussed below.

In order to analyze the temporal change in the absorption spectra quantitatively, we resolved the transient absorption spectra by using each spectrum of polymer hole polarons, PCBM radical anion, and PCBM radical cation. For blend films with 5 wt% PCBM, as shown in **Figure 4**a,c, the observed

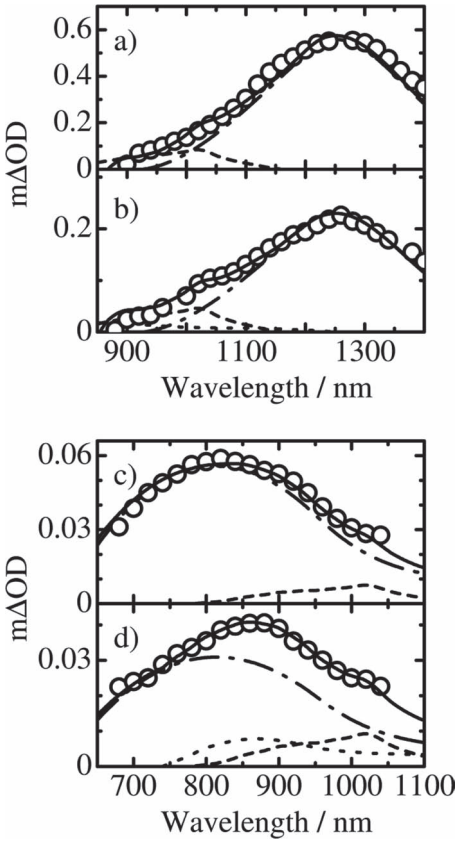

Figure 4. Transient absorption spectra of blend films (open circles) at 1 μs after the laser excitation at 400 nm with a fluence of 30 μJ cm^{-2}: a) PCPDTBT/PCBM (95:5 w/w), b) PCPDTBT/PCBM (50:50 w/w), c) N-P7/PCBM (95:5 w/w), and d) N-P7/PCBM (50:50 w/w). The solid lines represent the absorption spectra simulated by the sum of each absorption spectrum of charge carriers: polymer$^+$ (dashed-dotted lines), PCBM$^-$ (broken lines), and PCBM$^+$ (dotted lines). The mole fraction of each spectrum is as follows: polymer$^+$: PCBM$^+$: PCBM$^-$ = a) 50:0:50, b) 35:15:50, c) 50:0:50, and d) 30:20:50.

spectra were well reproduced by the sum of the absorption spectra of polymer hole polaron and PCBM radical anion. We therefore conclude that hole polaron and PCBM radical anion are formed as charge carriers in the blend films with 5 wt% PCBM. From the spectral simulation, the molar absorption coefficients of polymer hole polarons are estimated to be $\varepsilon_{PCPDTBT}{}^{+}$ = 40000 M^{-1} cm^{-1} at 1240 nm and $\varepsilon_{N\text{-}P7}{}^{+}$ = 40000 M^{-1} at 850 nm on the basis of that of PCBM radical anion $\varepsilon_{PCBM}{}^{-}$ = 6000 M^{-1} cm^{-1} at 890 nm.[13] This is larger than that of MDMO-PPV hole polaron ($\varepsilon_{MDMO\text{-}PPV}{}^{+}$ = 15000 M^{-1} cm^{-1}), but rather comparable to that of polythiophene hole polaron (ε = 34000 M^{-1} cm^{-1}).[13,25] Note that the charge density is typically 10^{16}–10^{17} cm^{-3}, which is comparable to that observed under the 1 sun open circuit condition.[26]

For blend films with 50 wt% PCBM, on the other hand, the transient spectra changed with time as shown in Figure 3. There are two possible explanations for the spectral change in polymer/PCBM blend films: i) the absorption spectrum of charge carriers (polymer hole polarons and/or PCBM radical anion) is dependent on the PCBM concentration and ii) the charge carrier composition is dependent on the PCBM concentration. As mentioned above, the absorption spectra of polymer hole polarons are independent on the dopant concentration. Furthermore, our previous study has demonstrated that the absorption spectrum of PCBM radical anion is also essentially independent of the PCBM concentration.[13] We therefore assigned that another charge carrier is formed in blend films at high PCBM concentrations. To explain the spectral change, we consider PCBM radical cation as the most possible carrier formed in blends at high PCBM concentrations. In contrast to the blend films with 5 wt% PCBM, the absorption spectra of the blend films with 50 wt% of PCBM were not reproducible by the sum of each spectrum of polymer hole polaron and PCBM radical anion. Rather, as shown in Figure 4b,d, the whole spectra observed at 1 μs were well reproduced by the sum of each spectrum of polymer hole polaron, PCBM radical anion, and PCBM radical cation. Thereafter, no spectral change was observed, suggesting that thermodynamic equilibrium is established. We therefore conclude that PCBM radical cation is formed with time in the blend films with 50 wt% PCBM. On the basis of the molar absorption coefficient of each carrier, the equilibrium fraction of PCBM radical cation formed in the blend films can be quantitatively evaluated to be F_{eq} = 0.3 for PCPDTBT and F_{eq} = 0.6 for N-P7 blend films at 1 μs.

The spectral changes before the thermodynamic equilibrium were well reproduced by the sum of each spectrum of polymer hole polaron, PCBM radical anion, and PCBM radical cation with different fractions. **Figure 5** shows the time dependence of the fraction $F(t)$ of PCBM radical cation in the blend films. The time evolution of $F(t)$ was well fitted with an exponential function: $F(t) = a[1-\exp(-t/\tau)]$. As a result, the time constant of the PCBM radical cation formation is estimated to be τ = 450 ns for PCPDTBT/PCBM and τ = 15 ns for N-P7/PCBM blend films. These rise constants are in good agreement with the decay constants of polymer hole polarons, suggesting that PCBM radical cations are formed from polymer hole polarons.

The hole injection from polymer to PCBM domains should be dependent on phase-separated domain size. We therefore analyzed the formation time of PCBM radical cation in PCPDTBT/PCBM blend films fabricated with 1,8-diiodooctane (DIO) as an additive for the spincast solution. The averaged domain size was evaluated to be 59 nm by AFM measurements, which is larger than 31 nm evaluated for PCPDTBT/PCBM blend films fabricated without DIO (see the Supporting Information). This additive effect is consistent with previous reports.[27–29] We note that the phase-separated polymer domain is not pure but contains PCBM molecules because polymer fluorescence is highly quenched for both films. We also note that the additive has no impact on the HOMO level of PCPDTBT in the blend. As shown in the open squares in Figure 5, the formation time of PCBM radical cation is ~2 μs, which is slower than that observed for PCPDTBT/PCBM blend films fabricated without DIO. The final fraction of PCBM radical cation is F_{eq} = 0.3, which is the same as that observed for the blend films fabricated without DIO. These results also suggest the hole injection from polymer to PCBM domains.

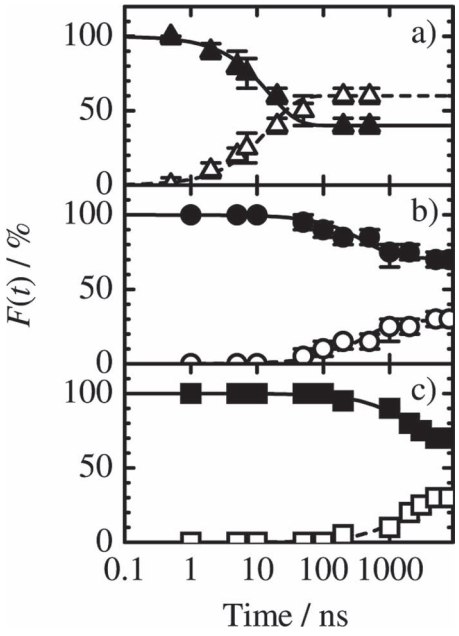

Figure 5. Time evolution of the mole fraction of PCBM radical cation (open symbols) and polymer polarons (closed symbols) to the total hole carriers in blend films: a) N-P7/PCBM, b) PCPDTBT/PCBM fabricated without DIO, and c) PCPDTBT/PCBM fabricated with DIO. The solid and broken lines show the fitting curves by $F(t) = a[1-\exp(-t/\tau)]$ (solid lines) and $F(t) = b\exp(-t/\tau)$ (broken lines).

2.2. Monte Carlo Simulation

To address the origin of the hole injection from polymer to PCBM domains, we simulated hole hopping in a semi-infinite donor/acceptor planar heterojunction by the Monte Carlo analysis. The calculation is based on the Miller–Abraham model for hopping in a disordered material.[30,31] In this model, the hopping probability P_{ij} from site i to site j is given by

$$P_{ij} = \frac{\nu_{ij}}{\sum_{l} \nu_{il}} \quad (1)$$

$$\nu_{ij}(\Delta E_{ij}) = \begin{cases} \exp\left(\frac{-\Delta E_{ij}}{k_B T}\right) \text{ for } \Delta E_{ij} > 0 \\ 1 \text{ for } \Delta E_{ij} \leq 0 \end{cases} \quad (2)$$

where ΔE_{ij} is the energy difference between site i and j, k_B is the Boltzmann constant, and T is temperature. All the site energy is generated randomly on the basis of the following Gaussian distribution function $D(E)$[32]

$$D_X(E) = \frac{d_X}{\sqrt{2\pi}\sigma_X} \exp\left[-\frac{(E - E_X^0)^2}{2\sigma_X^2}\right] \quad (3)$$

where E_X^0 is the HOMO energy level of the domain X, d_X is the degeneracy in the HOMO levels of the domain X, σ_X is the width of the energetic Gaussian distribution of the HOMO levels for the domain X, and the subscripts of D and A stand for donor and acceptor, respectively. The HOMO energy E_X^0 is evaluated by the photoelectron yield spectroscopy. Here, we set $d_A = 5$ for PCBM, which has fivefold degeneracy in the HOMO levels,[33] and $d_D = d_A = 1$ for polymers. The width σ_X is taken from previous studies. For most conjugated polymer films, the width due to energetic disorders has been reported to be around 0.1 eV.[34–42] Thus, we set $\sigma_D = \sigma_A = 0.1$ eV for polymers as a typical value. For fullerene and its derivatives, the band width (full width half mean) has been reported to range from 0.8 to 1.1 eV.[43–50] Thus, we set $\sigma_A = 0.4$ eV for PCBM as a minimum value. In the simulation, a hole is generated at one of the nearest neighbor sites at the heterojunction. The hole is iteratively hopping in a simple cubic lattice: it moves from a site i to an adjacent site j with a probability of P_{ij} or stays at the original site with a probability of P_{ii}. It is determined whether the hole finally stays at the donor or acceptor domain. This calculation is independently performed for 3000 holes. As a result, the equilibrium fractions F_{eq} of holes in the acceptor domain is obtained as a function of ΔE_{HOMO}.

Figure 6 shows the simulation results with the typical parameters of a polymer/fullerene blend at a high fullerene fraction (σ_D = 0.1 eV, σ_A = 0.4 eV, d_A = 5), of a polymer/fullerene blend with a low fullerene fraction ($\sigma_D = \sigma_A = 0.1$ eV, $d_A = 5$), and of a polymer/polymer blend ($\sigma_D = \sigma_A = 0.1$ eV, $d_A = 1$). For the polymer/fullerene blend film with a high fullerene fraction, F_{eq} is as high as >0.9 for $\Delta E_{HOMO} < 0.5$ eV, steeply decreases at around $\Delta E_{HOMO} \approx 0.6$ eV, and then is as small as <0.2 for $\Delta E_{HOMO} > 0.8$ eV. For the polymer/fullerene blend film with a low fullerene fraction, on the other hand, F_{eq} is ~0.9 for $\Delta E_{HOMO} = 0$ eV, but steeply decreases, and then is negligibly small for $\Delta E_{HOMO} > 0.2$ eV, which is similar to the polymer/polymer blend films where F_{eq} is ~0.5 for $\Delta E_{HOMO} = 0$ eV, but F_{eq} is negligibly small for $\Delta E_{HOMO} > 0.1$ eV. This result shows that the distribution width in the HOMO energy has critical impact on the hole injection from polymer to fullerene domains. We will discuss the energetic conditions for holes injection into acceptor domains.

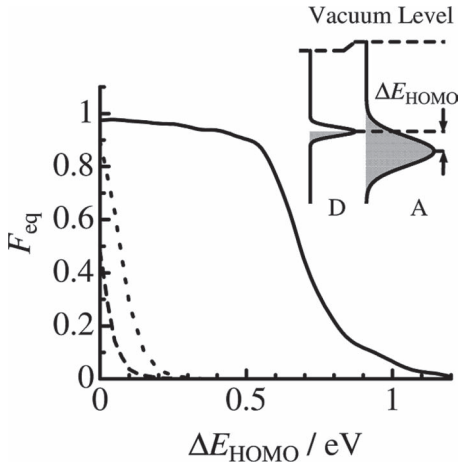

Figure 6. Equilibrium fraction of PCBM radical cation F_{eq} plotted against ΔE_{HOMO} calculated by the Monte Carlo simulation with the following parameters: σ_D = 0.1 eV, σ_A = 0.4 eV, d_D = 1, d_A = 5 (solid line) for a polymer/fullerene blend with a high fullerene fraction, $\sigma_D = \sigma_A$ = 0.1 eV, d_D = 1, d_A = 5 (dotted line) for a polymer/fullerene blend with a low fullerene fraction, and $\sigma_D = \sigma_A$ = 0.1 eV, $d_D = d_A$ = 1 (broken line) for a polymer/polymer blend. The inset shows the energy diagram of the HOMO levels.

3. Discussion

3.1. Formation Mechanism of PCBM Cation

In the previous study,[13] we proposed two possible mechanisms for the formation of the PCBM radical cation in blend films. One is the formation of the PCBM radical cation and anion pairs at the PCBM domain in the blend, which would be caused by the direct or indirect excitation of intermolecular CT transitions of PCBM. The other is the formation of the PCBM radical cation by hole injection from hole polarons in polymer domains. If the former mechanism were dominant, the PCBM radical cation should be observed immediately after the laser excitation and some of them would rapidly decay because of the geminate recombination. As shown in Figure 3, this is not the case. In reality, no PCBM radical cation is observed on a time scale of nanoseconds, but the fraction of PCBM radical cation rather increases with time in parallel with the decrease in the fraction of polymer polarons with the same time constant. Furthermore, if the former mechanism were dominant, the final fraction of the PCBM radical cation should be dependent on the excitation wavelength. This is also not the case as described above. These transient results strongly suggest the hole injection from polymer to PCBM domains. If the latter mechanism is dominant, the hole injection time should be dependent on the domain size. Indeed, we observed the different formation dynamics of PCBM radical cation in PCPDTBT/PCBM blend films with different phase-separated domain sizes: PCBM radical cation is generated faster (450 ns) in smaller domains (31 nm) but slower (2 μs) in larger domains (59 nm). Assuming that the hole mobility $\mu_h = 10^{-4}$ cm^2 V^{-1} s^{-1},[29,51,52] the diffusion constant of the hole carrier is calculated by the Einstein's relationship $D = (k_B T/q)\mu$ where q is the elementary charge. As a result, the 3D diffusion length $\langle x^2 \rangle^{1/2} = (6Dt)^{1/2}$ is estimated to be 25 nm for 450 ns and 55 nm for 2 μs, which are in good agreement with the domain sizes observed. On the basis of these findings, we therefore conclude that PCBM radical cation is formed mainly by the hole injection from polymer polarons in polymer domains.

3.2. Energetic Conditions

Next, we discuss the energetic conditions for the hole injection to acceptor domains even in polymer/fullerene blend films. As shown in Figure 1, the HOMO levels of all the conjugated polymers studied are higher than that of PCBM. In other words, hole carriers should be energetically more stable in conjugated polymers than in PCBM molecules in terms of the simple energetic scheme. Thus, it is necessary to consider energetic distribution in the HOMO levels or energetic realignment at the interface in order to explain the hole injection from polymer to PCBM domains. As mentioned above, most organic semiconductors exhibit energetic disorder in the range of 0.1 eV for charge transport.[34–42] However, as shown by the broken line in Figure 6, F_{eq} is negligible for the parameters ($\sigma_D = \sigma_A =$ 0.1 eV, $d_D = d_A = 1$), suggesting no hole injection from donor to acceptor domains. These parameters are typical for most polymer/polymer blends. In other words, the hole injection from donor to acceptor would be negligible for polymer/polymer blend films. On the other hand, as mentioned above, fullerene derivatives have fivefold degenerated HOMO levels ($d_A = 5$). As shown by the dotted line in Figure 6 ($\sigma_D = \sigma_A = 0.1$ eV, $d_D =$ 1, $d_A = 5$), F_{eq} is still negligible for $\Delta E_{HOMO} > 0.2$ eV. These parameters correspond to polymer/fullerene blends with low fullerene fractions because energetic distribution of isolated fullerenes would be dependent on the energetic disorder of the polymer matrix. Indeed, no hole injection from polymer to PCBM domains is observed for the blends with low PCBM fractions (<30 wt%). At a higher PCBM concentration, PCBM molecules are likely to form aggregated clusters or nanocrystals. As reported previously,[53] the intermolecular CT absorption band of PCBM at 500 nm becomes prominent at high PCBM concentrations, suggesting substantial intermolecular interaction in the ground state. Large intermolecular interactions generally cause crystallization, resulting in band structures in the electronic state. For C_{60} crystals, there are many studies on the band structure. The band width of the valence band has been estimated to be 0.8 to 1.2 eV by the photoemission spectra.[43–50] For PCBM, a recent calculation suggests that the simple cubic structure is most stable and causes a broadening of the energy levels resulting from the overlap of neighboring PCBM orbital due to the compact packing.[54] As shown by the solid line in Figure 6 ($\sigma_D = 0.1$ eV, $\sigma_A = 0.4$ eV, $d_D = 1$, $d_A = 5$), F_{eq} is as large as 0.9 for $\Delta E_{HOMO} < 0.5$ eV, start to decrease at around $\Delta E_{HOMO} \approx 0.6$ eV, and negligible for $\Delta E_{HOMO} > 0.8$ eV. This is qualitatively consistent with F_{eq} obtained from the transient measurements. Therefore, we conclude that the hole injection from polymer to PCBM domains is primarily due to the large band width of PCBM nanocrystals and secondarily due to the fivefold degeneracy in the HOMO levels of PCBM.

Finally we note the energy difference Δ between ΔE_{HOMO} and $E_A^0 - E_D^0$. As shown in **Figure 7**, the observed F_{eq} is different from the calculated for ΔE_{HOMO} with $\Delta = 0$, which corresponds to $E_A^0 - E_D^0$. The difference is $\Delta = 0.37$ eV for PCPDTBT/PCBM, $\Delta = 0.17$ eV for N-P7/PCBM, and $\Delta = 0.20$ eV for MDMO-PPV/PCBM. This is probably because other important factors are neglected in this simple simulation. For example, interfacial dipoles at the heterojunction have been reported to cause 0.2–0.6 eV of vacuum level shift.[55,56] Such interfacial dipoles have been found for many polymer/fullerene blend films: 0.4 eV for P3HT/PCBM,[57] 0.6 eV for P3HT/C_{60},[58] and 0.25 eV for PPV oligomer/C_{60}.[59] These values are comparable to the estimated Δ mentioned above, suggesting that most of Δ can be explained by the vacuum level shift.

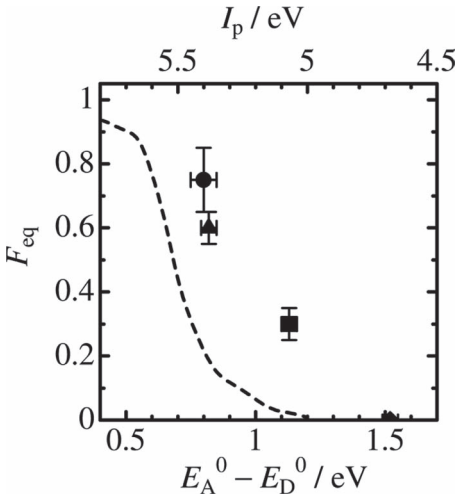

Figure 7. Equilibrium fraction of of PCBM radical cation F_{eq} obtained from the transient study plotted against $E_A^0 - E_D^0$ (lower axis) and I_p of conjugated polymers (upper axis): MDMO-PPV/PCBM (circle), N-P7/PCBM (triangle), PCPDTBT/PCBM (square), and P3HT/PCBM (diamond) blends. The broken line indicates the calculated F_{eq} with $\Delta = 0$ shown in Figure 6 for the polymer/fullerene blend with a high fullerene fraction.

4. Conclusions

The formation dynamics of PCBM radical cation in polymer/PCBM blends was studied by transient absorption measurements. As a result, we obtained the key findings as follows. At an early time stage after the photoexcitation, polymer hole polaron and PCBM radical anion were observed but no PCBM radical cation was found. On a time scale of nanoseconds, the fraction of PCBM radical cation increased with time while the fraction of polymer hole polaron decreased with the same time constant. Finally, the fraction of PCBM radical cation became constant on a time scale of microseconds, suggesting that thermodynamic equilibrium is established. The formation time of PCBM radical cation is dependent on the phase-separated domain sizes: the slower formation of PCBM radical cation was observed for the larger domains. The final fraction of PCBM radical cation F_{eq} is dependent on the ionization potential of donor polymers but independent of the domain size and the excitation wavelength: $F_{eq} = 30\%$ for PCPDTBT/PCBM and $F_{eq} = 60\%$ for N-P7/PCBM blends. We therefore conclude that PCBM radical cation is generated mainly by the hole injection from polymer to PCBM domains in polymer/PCBM blends. In order to discuss the energetic conditions for the hole injection to acceptor in donor/acceptor blends, we simulated hole hopping at donor/acceptor heterojunction by the Monte Carlo analysis based on the Miller–Abraham model. In this simulation, we consider the energetic distribution and the degeneracy in the HOMO levels. As a result, the hole injection would be negligible for polymer/

polymer blends because the energetic distribution is as small as 0.1 eV and the degeneracy is typically unity. Even for polymer/PCBM with the fivefold degeneracy in the HOMO of PCBM, the hole injection would be negligible for lower PCBM fractions because of the small energetic distribution. In contrast, the hole injection is energetically favorable for higher PCBM fractions because of the large band width due to the formation of aggregated PCBM nanocrystals and the fivefold degeneracy in the HOMO levels of PCBM. This is consistent with the final fraction obtained from the transient study. We therefore conclude that the hole injection from polymer to PCBM domains is primarily due to the large band width of PCBM nanocrystals and secondarily due to the fivefold degeneracy in the HOMO levels of PCBM. We believe that such conditions would be true for other polymer/fullerene solar cells in particular employing polymers with deeper HOMO levels.

5. Experimental Section

Materials: Chemical regents for PCPDTBT synthesis were used without further purification: 2,1,3-benzothiadiazole-4,7-bis(boronic acid pinacol ester) (Aldrich, 95%), 2,6-dibromo-4,4-bis(2-ethylhexyl)-4*H*-cyclopenta[2,1-b:3,4-b′]dithiophene (Luminescence Technology Corp.), potassium carbonate (Aldrich, 99.995%), Aliquat(R)336 (Aldrich, 99.995%), toluene (Wako, Organic synthesis grade), tetrakis(triphenylphosphine)palladium(0) (Aldrich, 99%), bromobenzene (Aldrich, >99.5%), and phenylboroic acid (Aldrich, >97.0%). Details of the synthesis of PCPDTBT are described in the Supporting Information. The other polymer N-P7 was provided by Toray Industries, Inc. The acceptor PCBM (99.9%) was purchased from Frontier Carbon and used without further purification. The other acceptor TCNB (98%) was purchased from Tokyo Chemical Industry Co., Ltd. and recrystallized from ethanol prior to the experiment.

Sample Fabrication: Polymer/fullerene blend films were prepared on glass substrates by spin-coating from a chlorobenzene solution of polymer and PCBM at a spin rate of 1000 rpm after the spin rate of 400 rpm (10 s) under ambient conditions. The film thickness was typically 200 nm. The weight fraction of PCBM was varied from 5 to 80 wt%. The blend solution was stirred at 40 °C overnight to be dissolved homogeneously. Before the spin-coating, the glass substrates were cleaned by ultrasonic treatment in toluene, acetone, and ethanol sequentially for 15 min each, and then with a UV-ozone cleaner (Nippon Laser & Electronics Lab., UV253) for 1 h. For blend films of polymer and TCNB, tetrahydrofuran (for PCPDTBT) or cyclohexanone (for N-P7) was used as solvent instead of chlorobenzene. The blend solution was stirred at room temperature over night. The weight fraction of TCNB was adjusted to 5 and 30 wt% in the final films.

Measurements: Transient absorption data were collected under N_2 atmosphere with a highly sensitive a nano/microsecond transient absorption system and with a femtosecond transient absorption system as described below. For the microsecond transient absorption measurement, the sample was excited with a light pulse (400 nm, 30 μJ cm^{-2}, 4 Hz) from a dye laser (Photon Technology International, GL-301) that was pumped with a nitrogen laser (Photon Technology International, GL-3300), and probed with a monochromatic light from a 50-W quartz tungsten halogen lamp (Thermo–ORIEL, Model 66997) with a light intensity controller (Thermo–ORIEL, Model 66950), which was equipped with appropriate optical cut-filters and two monochromators (Ritsu, MC-10N) before and after the sample to reduce stray light, scattered light, and emission from the sample. The probe light was detected with a pre-amplified Si photodiode (Costronics Electronics) for the visible wavelength range from 700 to 1100 nm or a pre-amplified InGaAs photodiode (Newport 1811) for the near-IR wavelength range from 900 to 1500 nm. The detected signal was sent to the main amplification system with electronic band-pass filters (Costronics Electronics) to improve the noise-to-signal ratio. The amplified signal was collected with a 200-MHz digital oscilloscope (Tektronix, TDS2022), which was synchronized with a trigger signal of the laser pulse from a photodiode (Thorlabs, DET10A). The detectable absorbance change ΔOD is as small as ~10^{-5}–10^{-6} depending on the measuring time region. For the nanosecond time region, the optical line was the same as the microsecond spectrometer mentioned above. The probe light was detected with a pre-amplified Si photodiode (Newport, 1801) for visible region or a pre-amplified InGaAs photodiode (Newport, 1811) for the near-IR region. The detected signal was amplified with a voltage amplifier (Femto, DHPVA-200) and collected with a 500-MHz digital oscilloscope (Tektronix, TDS3052B). The femtosecond transient absorption data were collected with a pump and probe transient absorption spectroscopy system (Ultrafast Systems, Helios). The pump light was second harmonic pulses (400 nm, 30 μJ cm^{-2}, fwhm 100 fs, 1 kHz) from a regeneratively amplified Ti-sapphire laser (Spectra-Physics, Hurricane). The probe beam was detected with a linear CMOS array (Ultrafast Systems, SPEC-VIS) for the visible wavelength range from 400 to 900 nm and with an InGaAs linear diode array (Ultrafast Systems, SPEC-NIR) for the near-IR wavelength range from 850 to 1600 nm. The typical noise level of this system is lower than 2×10^{-4}.

Supporting Information

Supporting Information is available from the Wiley Online Library or from the author.

Acknowledgements

The authors thank the Toray Industries, Inc. for providing the N-P7 used in this experiment. This work was partly supported by the JST PRESTO program (Photoenergy Conversion Systems and Materials for the Next Generation Solar Cells), the JSPS Research Fellowship for Young Scientists, and the Global COE program (International Center for Integrated Research and Advanced Education in Materials Science) from the Ministry of Education, Culture, Sports, Science, and Technology, Japan.

Received: January 11, 2012
Revised: February 28, 2012
Published online: April 17, 2012

[1] P. Heremans, D. Cheyns, B. P. Rand, *Acc. Chem. Res.* **2009**, *42*, 1740.
[2] B. Kippelen, J.-L. Brédas, *Energy Environ. Sci.* **2009**, *2*, 251.
[3] J. Zaumseil, H. Sirringhaus, *Chem. Rev.* **2007**, *107*, 1296.
[4] E. J. Meijer, D. M. de Leeuw, S. Setayesh, E. van Veenendaal, B.-H. Huisman, P. W. M. Blom, J. C. Hummelen, U. Scherf, T. M. Klapwijk, *Nat. Mater.* **2003**, *2*, 678.
[5] T. Yasuda, T. Goto, K. Fujita, T. Tsutsui, *Appl. Phys. Lett.* **2004**, *85*, 2098.
[6] T. D. Anthopoulos, C. Tanase, S. Setayesh, E. J. Meijer, J. C. Hummelen, P. W. M. Blom, D. M. de Leeuw, *Adv. Mater.* **2004**, *16*, 2174.
[7] L.-L. Chua, J. Zaumseil, J.-F. Chang, E. C.-W. Ou, P. K.-H. Ho, H. Sirringhaus, R. H. Friend, *Nature* **2005**, *434*, 194.
[8] E. C. P. Smits, T. D. Anthopoulos, S. Setayesh, E. Van Veenendaal, R. Coehoorn, P. W. M. Blom, B. De Boer, D. M. De Leeuw, *Phys. Rev. B* **2006**, *73*, 205316.
[9] H. Sirringhaus, *Nature* **2009**, *457*, 667.
[10] C. Melzer, E. J. Koop, V. D. Mihailetchi, P. W. M. Blom, *Adv. Funct. Mater.* **2004**, *14*, 865.

[11] S. M. Tuladhar, D. Poplavskyy, S. A. Choulis, J. R. Durrant, D. D. C. Bradley, J. Nelson, *Adv. Funct. Mater.* **2005**, *15*, 1171.
[12] A. Gadisa, K. Tvingstedt, K. Vandewal, F. Zhang, J. V. Manca, O. Inganäs, *Adv. Mater.* **2010**, *22*, 1008.
[13] S. Yamamoto, J. Guo, H. Ohkita, S. Ito, *Adv. Funct. Mater.* **2008**, *18*, 2555.
[14] J. Y. Kim, K. Lee, N. E. Coates, D. Moses, T.-Q. Nguyen, M. Dante, A. J. Heeger, *Science* **2007**,*317*, 222.
[15] D. Kitazawa, N. Watanabe, S. Yamamoto, J. Tsukamoto, *J. Photopolym. Sci. Technol.* **2010**, *23*, 293.
[16] B. C. Thompson, J. M. J. Fréchet, *Angew. Chem. Int. Ed.* **2008**, *47*, 58.
[17] J. Peet, J. Y. Kim, N. E. Coates, W. L. Ma, D. Moses, A. J. Heeger, G. C. Bazan, *Nat. Mater.* **2007**, *6*, 497.
[18] D. Kitazawa, N. Watanabe, S. Yamamoto, J. Tsukamoto, *Appl. Phys. Lett.* **2009**, *95*, 053701.
[19] J. K. J. Duren, X. Yang, J. Loos, C. W. T. Bulle-Lieuwma, A. B. Sieval, J. C. Hummelen, R. A. J. Janssen, *Adv. Funct. Mater.* **2004**, *14*, 425.
[20] A. Tsuchida, M. Yamamoto, Y. Nishijima, *J. Phys. Chem.* **1984**, *88*, 5062.
[21] D. M. Guldi, M. Prato, *Acc. Chem. Res.* **2000**, *33*, 695.
[22] I.-W. Hwang, C. Soci, D. Moses, Z. Zhu, D. Waller, R. Gaudiana, C. J. Brabec, A. J. Heeger, *Adv. Mater.* **2007**, *19*, 2307.
[23] T. Clarke, A. Ballantyne, F. Jamieson, C. Brabec, J. Nelson, J. Durrant, *Chem. Commun.* **2009**, 89.
[24] S. Fukuzumi, H. Mori, H. Imahori, T. Suenobu, Y. Araki, O. Ito, K. M. Kadish, *J. Am. Chem. Soc.* **2001**, *123*, 12458.
[25] J. Guo, H. Ohkita, S. Yokoya, H. Benten, S. Ito, *J. Am. Chem. Soc.* **2010**, *132*, 9631.
[26] A. Maurano, R. Hamilton, C. G. Shuttle, A. M. Ballantyne, J. Nelson, B. O'Regan, W. Zhang, I. McCulloch, H. Azimi, M. Morana, C. J. Brabec, J. R. Durrant, *Adv. Mater.* **2010**, *22*, 4987.
[27] A. Moulé, K. Meerholz, *Adv. Funct. Mater.* **2009**, *19*, 3028.
[28] J. K. Lee, W. L. Ma, C. J. Brabec, J. Yuen, J. S. Moon, J. Y. Kim, K. Lee, G. C. Bazan, A. J. Heeger, *J. Am. Chem. Soc.* **2008**, *130*, 3619.
[29] M. Dante, A. Garcis, T.-Q. Nguyen, *J. Phys. Chem. C* **2009**, *113*, 1596.
[30] A. Miller, E. Abrahams, *Phys. Rev.* **1960**, *120*, 745.
[31] N. Tessler, Y. Preezant, N. Rappaport, Y. Roichman, *Adv. Mater.* **2009**, *21*, 2741.
[32] G. Garcia-Belmonte, J. Bisquert, *Appl. Phys. Lett.* **2010**, *96*, 113301.
[33] H. W. Kroto, A. W. Allaf, S. P. Balm, *Chem. Rev.* **1991**, *911*213.
[34] H. Bässler, *Phys. Status Solidi (b)* **1993**, *175*, 15.
[35] C. Tanase, P. W. M. Blom, D. M. De Leeuw, E. J. Meijer, in *Physics of Organic Semicondutors* (Ed: W. Brütting), Wiley-VCH, Weinheim, Germany **2005**.
[36] P. W. M. Blom, M. C. J. M. Vissenberg, *Mater. Sci. Eng.* **2000**, *27*, 53.
[37] W. Tang, V. Chellappan, M. Liu, Z.-K. Chen, L. Ke, *ACS Appl. Mater. Interfaces* **2009**, *1*, 1467.
[38] L. M. Anderson, W. Osikowicz, F. L. E. Jakobsson, M. Berggren, L. Lindgren, M. R. Anderson, O. Inganäs, *Org. Electron.* **2008**, *9*, 569.
[39] F. Laquai, G. Wegner, C. Im, H. Bässler, S. Heun, *Appl. Phys. Lett.* **2006**, *99*, 023712.
[40] A. M. Ballantyne, L. Chen, J. Dane, T. Hammant, F. M. Braun, M. Heeney, W. Duffy, I. McCulloch, D. D. C. Bradley, J. Nelson, *Adv. Funct. Mater.* **2008**, *18*, 2373.
[41] I. I. Fishchuk, A. K. Kadashchuk, J. Genoe, M. Ullah, H. Sitter, Th. B. Singh, N. S. Sariciftci, H. Bässler, *Phys. Rev. B* **2010**, *81*, 045202.
[42] Y. Zhang, P. W. M. Blom, *Appl. Phys. Lett.* **2011**, *98*, 143504.
[43] M. S. Golden, M. Knupfer, J. Fink, J. F. Armbruster, T. R. Cummins, H. A. Romberg, M. Roth, M. Sing, M. Schmidt, E. Sohmen, *J. Phys.: Condens. Matter.* **1995**, *7*, 8219.
[44] W. Y. Ching, M.-Z. Huang, Y.-N. Xu, W. G. Harter, F. T. Chan, *Phys. Rev. Lett.* **1991**, *67*, 2045.
[45] E. L. Shirley, S. G. Louie, *Phys. Rev. Lett.* **1993**, *71*, 133.
[46] M. Merkel, M. Knupfer, M. S. Goldewn, J. Fink, R. Seemann, R. L. Johnson, *Phys. Rev. B* **1993**, *47*, 11470.
[47] P. J. Benning, C. G. Olson, D. W. Lynch, J. H. Weaver, *Phys. Rev. B* **1994**, *50*, 11239.
[48] G. K. Wertheim, *Phys. Rev. B* **1995**, *51*, 10248.
[49] K. Akaike, K. Kanai, H. Yoshida, J. Tsutsumi, T. Nishi, N. Sato, Y. Ouchi, K. Seki, *J. Appl. Phys.* **2008**, *104*, 023710.
[50] Q. Wei, K. Tajima, Y. Tong, S. Ye, K. Hashimoto, *J. Am. Chem. Soc.* **2009**, *131*, 17597.
[51] M. Lenes, M. Morana, C. J. Brabec, P. W. M. Blom, *Adv. Funct. Mater.* **2009**, *19*, 1106.
[52] C.-H. Chen, C.-H. Hsieh, M. Dubosc, Y.-J. Cheng, C.-S. Hsu, *Macromolecules* **2010**, *43*, 697.
[53] S. Cook, H. Ohkita, Y. Kim, J. J. Benson-Smith, D. D. C. Bradley, J. R. Durrant, *Chem. Phys. Lett.* **2007**, *445*, 276.
[54] J. M. N.-Duarte, M. R.-Reyes, J. L. R.-Chavez, R. G.-Alonso, R. L.-Sandoval, *Phys. Rev. B* **2008**, *78*, 035425.
[55] H. Ishii, K. Sugiyama, E. Ito, K. Seki, *Adv. Mater.* **1999**, *11*, 605.
[56] S. Braun, W. R. Salaneck, M. Fahlman, *Adv. Mater.* **2009**, *21*, 1450.
[57] Z. Xu, L.-M. Chen, M.-H. Chen, G. Li, Y. Yang, *Appl. Phys. Lett.* **2009**, *95*, 013301.
[58] W. Osikowicz, M. P. de Jong, W. R. Salaneck, *Adv. Mater.* **2007**, *19*, 4213.
[59] S. C. Veenstra, H. T. Jonkman, *J. Polym. Sci. B* **2003**, *41*, 2549.